# A COMPARATIVE DESIGN ANALYSIS OF TRANSURANIC BURNER CORES WITH LOW SODIUM VOID REACTIVITY

Sang Ji Kim* and Nam Zin Cho
Department of Nuclear Engineering
Korea Advanced Institute of Science and Technology
373-1 Kusong-dong, Yusong-gu, Taejon, Korea 305-701
sjkim3@kaeri.re.kr ; nzcho@sorak.kaist.ac.kr

Young Jin Kim
Korea Atomic Energy Research Institute
150 Dukjin-dong, Yusong-gu, Taejon, Korea 305-353
youkim@kaeri.re.kr

## ABSTRACT

This study summarizes the neutronic performance and fuel cycle behavior of three geometrically-different transuranic (TRU) burner cores with similar low sodium void reactivity. These cores encompass a two-region homogeneous core, an annular core and a pan-shape core. Three different conceptual cores are designed with the same assembly specifications and managed to have similar end-of-cycle sodium void reactivities and beginning-of-cycle peak power densities through the changes in the core size and configuration. The requirement of low sodium void reactivity is shown to lead each design concept to characteristic neutronics performance and fuel cycle behavior. The merits of each design are different among the designs and the "best" core concept depends on the given situation. The pan-shape core is shown to have many attractive features over the other two designs, except for higher TRU feed enrichment. One notable advantage of the annular core and the pan-shape core is that the maximum three dimensional pin peak can be controlled even with a single enrichment, essentially eliminating the requirement of enrichment control. They only need the blending of fissile material with fertile material for the uniform enrichment fuels, which in turn may open the environmentally benign new reprocessing technology and eliminate the international barriers on the deployment of liquid metal reactor (LMR) cores.

## 1. INTRODUCTION

The primary concern of the radioactive nuclide management has been given to TRU nuclides in the form of irradiated fuel assemblies in Light Water Reactor (LWR) spent fuel pools. Earlier studies have shown that the greater long-term safety could be achieved in the disposal of high-level wastes if actinides are separated from fission products and burned in power reactors. Feasibility studies of actinide transmutation

---
*current address : Korea Atomic Energy Research Institute

in power reactors have shown that a LMR offers an advantage because of a preferential fission to capture reaction ratio in the hardened neutron spectrum environment.

The positive sodium void reactivity has long been one of the main safety problems of sodium cooled fast reactors. The functional requirement of the LMR for treating minor actinides (MA) has accelerated the study on LMR design options to make the sodium void reactivity negative. Consequently, numerous strategies for TRU burning with low sodium void reactivies[1-5] have been proposed for the contemporary worldwide need. As one of TRU burner cores, we devised the pan-shape core design with a variable core height[6] and its functionality to reduce the TRU contained in the PWR spent fuel has been analyzed. Since different organizations focused on different designs, each core design feature is analyzed in a significant detail and the parametric studies of composition change effects on the sodium void reactivity have been investigated for any given reference design. However, it is noted that the independently developed designs have rarely been compared with the same core power rating and design criteria. Considering that the spoiled geometry of TRU burner cores and rarely verified MA cross section impose large uncertainties on any computer code system in use, this study aims to develop various TRU burner cores with the same design methodology and the same design criteria only through core size and shape modifications without adjusting assembly structure. This research would be able to finally pinpoint the advantages and disadvantages of each core concept, independent of the accuracy of any specific code system.

## 2. ANALYSIS METHODOLOGY

Nuclear predictions start from the generation of regionwise microscopic cross sections, based on the Bondarenko self-shielding factor method. An 80-group neutron cross section library version, KAFAX[7], is prepared in the MATXS library format, based on the JEF-2.2 nuclear data files. The regionwise microscopic cross-section sets for 9-groups are generated by utilizing the effective cross section generation module composed of TRANSX[8] and TWODANT[9]. The data processing in this module includes resonance and spatial self-shielding corrections, reactor and cell flux solutions and cross section group collapsing. The neutron spectra necessary for group collapsing are obtained from the $P_3S_8$ transport theory calculations in a two-dimensional, coarse meshed RZ model with the TWODANT code.

Fuel cycle analysis consists of an in-reactor cycle, including the neutron flux equation, burnup and system constraints, and an external cycle simulating reprocessing, fabrication of new fuel assemblies, and preloading stages. These calculations are carried out with REBUS-3[10] in the equilibrium cycle. The equilibrium cycle approach approximates reactor characteristics after many cycles of operation subject to a fixed, repetitive fuel management strategy, and thus provides an efficient tool for the conceptual design study. The charge fuels can be reprocessed fuels modified by the external feeds or may be loaded from external feeds alone. These calculations are performed with all the control rods withdrawn. No contamination of recovered TRU by fission products is assumed in this study.

Since a significant amount of MA exists in the reactor core, the burnup and decay chain of actinides in the REBUS-3 model is extended from the one typically used for the fast breeder reactor analysis. The depletion and decay chain modeled in this study contains 14 explicit TRU nuclides and total of 18 actinides.

Reactivity coefficients are determined by two successive flux computations for the unperturbed and perturbed cores, utilizing the triangular-z finite difference diffusion option of DIF3D[11] with respective 9-group cross-sections. Radial 24 triangles per assembly are modeled and the axial mesh size is halved from that of the equivalent nodal model for fuel cycle analysis. BOEC and EOEC specific nuclide densities are extracted from the files saved during the REBUS-3 fuel cycle analysis. The flooded core has a nominal

temperature and coolant density. In the voided configuration, the flowing sodium was removed along the fueled assemblies, including the driver fuel, upper fission gas plenum, lower reflector and lower shield. The isothermal temperature coefficient of fueled assemblies is evaluated from the difference between the nominal temperature and the elevated temperature by 300K in the active core.

## 3. CORE DESIGN DESCRIPTIONS

The three conceptual core designs are depicted in Figure 1. The annular core is developed in reference 2. Its core power rating is 1575 MWt and U-Pu-10Zr metallic fuel is used. Since this core has served as the '96 OECD/NEA international benchmark core[5], many organizations have gathered some experience with it and the designers are familiar with its characteristic behavior. Two other design concepts for the performance and sodium void reactivity comparison are the two-region homogeneous core developed in this study and the pan-shape core of reference 6. Since the pan-shape core was designed to have the most negative sodium void reactivity, this core is slightly modified to result in the same void reactivity, which is accompanied with a reduction in the number of fuel assemblies. These two cores are developed to meet the core power level, maximum three dimensional peak at the beginning of equilibrium cycle (BOEC) and whole core sodium void reactivity at the end of equilibrium cycle (EOEC) observed in the annular core. The fuel assembly and other non-power producing assembly specifications inherit the simplified model of the benchmark problem in reference 5, except that the fuel enrichments are distinctive for each design.

The main mechanism of three design concepts to achieve low sodium void reactivity, is identically via the core pancaking which enhances axial neutron leakage upon the formation of sodium void. A supplementary way of reducing the sodium void reactivity is different among design concepts. The annular core places a central reflector/$B_4C$ island for the additional reduction of sodium void reactivity. The homogeneous core further reduces the core H/D ratio and requires two enrichment zones for the power distribution flattening in order to limit the increase of the core diameter. The pan-shape core has a maximum pancaking in the inner core, while longer outer core fuels compensate for the small power sharing of shorter inner core fuels.

The three core designs have the maximum three dimensional peak power density less than 460 W/cm at the beginning of the equilibrium cycle, and the flowing sodium voiding axially throughout the driver fuel assemblies is to produce about $-0.5\%\Delta\rho$ sodium void reactivity. Each core geometry is finalized by the sodium void reactivity at EOEC, since this is the time when the sodium void reactivity is least negative.

The relevant fuel cycle assumptions for the core neutronic evaluation are given in Table I. The isotopic compositions of LWR discharged TRU in Table II are used as external feed Pu and MA compositions for charge fuel fabrication mainly consisting of self-recycled TRU. The fuel cycle assumptions and isotopic compositions apply to all three reactor designs.

Table I. Fuel cycle assumptions

| | | |
|---|---|---|
| Reactor Power (MWt) | 1575 | 1575 |
| Cycle Length (days) | 365 | 548 |
| Capacity Factor (%) | 85 | 85 |
| Refueling Batches | 3,4 | 4 |
| Cooling Time (year) | | |
| LWR Discharge | 3.17 | 3.17 |
| TRU Burner Discharge | 1 | 1.5 |
| Reprocessing Time (month) | 6 | 9 |
| Refabrication Time (month) | 6 | 9 |
| TRU Recovery Factor | 1.0 | 1.0 |

Table II. LWR transuranic isotopes after 3.17 year cooling

| Isotope | Wt fraction | Isotope | Wt fraction |
|---|---|---|---|
| Pu-238 | 1.01E-02 | Np-237 | 5.40E-02 |
| Pu-239 | 0.508 | Am-241 | 2.51E-02 |
| Pu-240 | 0.199 | Am-242m | 1.11E-04 |
| Pu-241 | 0.134 | Am243 | 2.48E-02 |
| Pu-242 | 3.88E-02 | Cm-242 | 9.73E-06 |
| | | Cm-243 | 7.86E-05 |
| | | Cm-244 | 5.52E-03 |
| | | Cm-245 | 5.08E-04 |
| | | Cm-246 | 6.31E-05 |

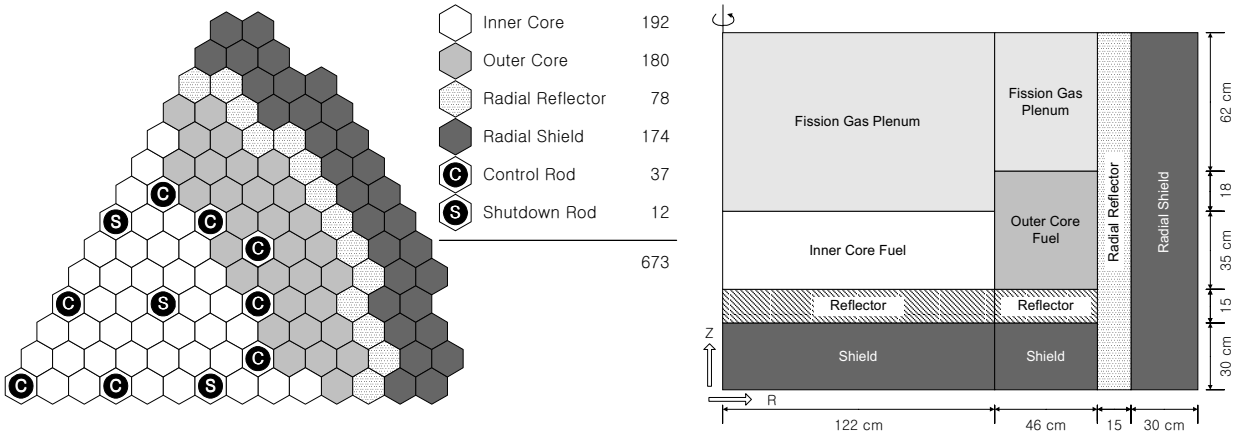


Pan-Shape Core

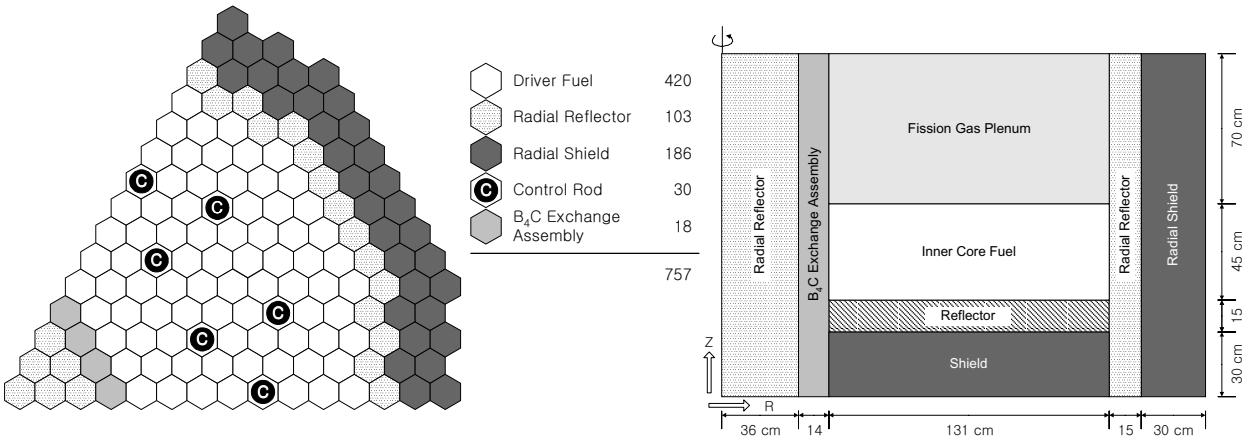


Annular Pancake Core

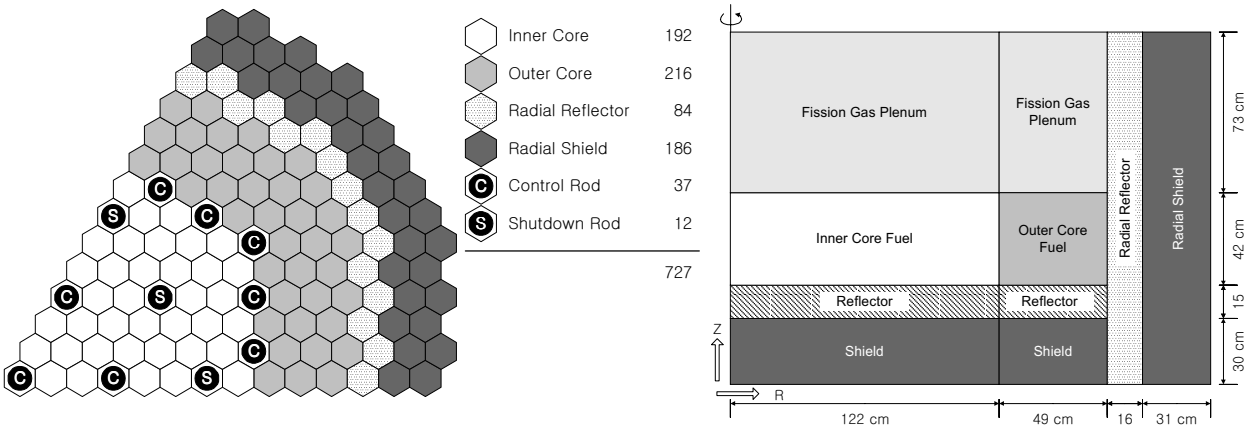


Homogeneous Core

Figure 1. Layout of Conceptual Core Designs for Design Comparisons

# 4. RESULTS OF ANALYSIS

## 4.1 NEUTRONIC PERFORMANCE CHARACTERISTICS

The evaluation of nuclear performance parameters and TRU mass flow data in the equilibrium cycle of each reactor core are carried out and summarized in Table IV for annual 3-batch, annual 4-batch and 18 month 3-batch operations. For a pre-determined fuel cycle option, the EOEC criticality with all rods out was achieved by the adjustment of charged fuel enrichment.

The burnup reactivity swings more than 4 %$\Delta\rho$ for any case incur large reactivity hold down requirement at BOEC. This is achieved by the control rods dispersed all over the core. A large number of control rod positions provided in the homogeneous and pan-shape core, is intended to allow a shallow insertion at BOEC and to give an eventual smaller ejected rod worth at hot full power. The TRU conversion ratios between 0.32 and 0.37 for the homogeneous and pan-shape cores suggest that the TRU destruction rate by fission reactions is about three times larger than the TRU production rate due to absorption reactions in U-236 and U-238. The high recycled TRU fraction for the annular core manifests that the net TRU burning during the depletion is the smallest among the three core layouts.

The peak linear heat generation rate is always less than 460 W/cm for any batch, cycle length and core layout. The remarkably stable ratio of peak to average power densities of the pan-shape and annular core for differing cycle length and fuel batches lead to the conclusion that for any charge enrichment, the two core layouts are assured to find out a reasonable fuel cycle scheme without significant core design alteration such as flow regrouping or the adjustment of core protection system setpoint. The low power peaking factor of the pan-shape core allowed envisaging the increase in the core average power density. This resulted in the active core volume reduction of 13.6% and 3.0%, compared with the annular core and the homogeneous core, respectively. The pan-shape core also shows the reduction of 36 driver fuel assemblies over the two-region homogeneous core, which should appear in the savings of assembly fabrication cost.

The peak fast fluence is highest for the annular core and this is related with the use of low enrichment fuels. The 18-month cycle operation is problematic for all the three core configurations and the problem is most significant for the annular core. Since the fast fluence limit is set by the displacement per atom (dpa) limit of the fuel clad, the evaluation of clad dpa by its own flux spectrum history is desirable to alleviate exceeding the fast fluence limit.

The average TRU enrichment of charged fuels is increasing from the annular core to the homogeneous core, and then to the pan-shape core. This ordering reflects that the active core volume decreases in the same order. This is basically related with the core design development process. The small 3-dimensional pin peak of the pan-shape core allows the compact core design which naturally requires a higher charge enrichment of Pu carrying MA, and the still low sodium void reactivity is accomplished by the high axial leakage throughout the inner core region. The pan-shape TRU burner core with a more negative sodium void reactivity and a higher TRU burning potential can be devised by increasing the inner core fuel assembly fraction when the active core volume of the annular core is to be kept. For the homogeneous core, it was found out during the core design survey that there is no room for the further sodium void reactivity reduction because the core is already extremely pancaked and the core is decoupled between the inner core and the outer core. Its power distribution is double-peaked in both the inner core and the outer core, and thus a small perturbation in either inner or outer core region tends to lead to a high radial peak in the other region. In contrast, the annular core is single-peaked toward the central annulus ring. A slightly more negative target sodium void reactivity may have not allowed any homogeneous core design possible.

Table III. Nuclear Performance Parameters and TRU Mass Flow Data

| Core Type | Pan-Shape | | | Annular | | | Homogeneous | | |
|---|---|---|---|---|---|---|---|---|---|
| Number of Cycles (Batches) | 3 | 3 | 4 | 3 | 3 | 4 | 3 | 3 | 4 |
| Cycle Length (month) | 12 | 18 | 12 | 12 | 18 | 12 | 12 | 18 | 12 |
| Burnup Reactivity Swing(%Δρ) | 4.7 | 7.2 | 4.8 | 4.2 | 6.4 | 4.31 | 4.4 | 6.7 | 4.5 |
| TRU Conversion Ratio | 0.35 | 0.32 | 0.34 | 0.42 | 0.38 | 0.41 | 0.37 | 0.33 | 0.35 |
| Recycled TRU Fraction | 0.84 | 0.76 | 0.79 | 0.86 | 0.79 | 0.81 | 0.84 | 0.77 | 0.79 |
| Average Discharge Burnup (MWdkg) | 93 | 140 | 125 | 82 | 123 | 110 | 91 | 136 | 121 |
| Peak Discharge Burnup (MWd/kg) | 124 | 185 | 164 | 122 | 178 | 160 | 122 | 180 | 160 |
| Core Average Linear Heat Rate (W/cm) | | 343 | | | 302 | | | 333 | |
| Peak Linear Power (W/cm) | | | | | | | | | |
| BOEC | 458 | 455 | 455 | 460 | 451 | 450 | 458 | 453 | 450 |
| EOEC | 454 | 453 | 453 | 439 | 424 | 431 | 436 | 432 | 434 |
| Power Peaking Factor | | | | | | | | | |
| BOEC | 1.33 | 1.32 | 1.32 | 1.52 | 1.49 | 1.49 | 1.37 | 1.36 | 1.35 |
| EOEC | 1.32 | 1.32 | 1.32 | 1.45 | 1.40 | 1.42 | 1.31 | 1.30 | 1.30 |
| Peak Fast Fluence ( $x10^{23}$ $n/cm^2$) | 2.64 | 3.91 | 3.53 | 2.91 | 4.22 | 3.83 | 2.66 | 3.91 | 3.56 |
| Charge Fuel TRU Enrichment (w/o) | 36.1 | 39.6 | 37.6 | 31.8 | 34.7 | 33.0 | 37.7 | 41.1 | 39.1 |
| Driver Assembly Number | | 372 | | | 420 | | | 408 | |
| Total Assembly Number | | 673 | | | 757 | | | 727 | |
| Active Core Volume (cc) | | 585489 | | | 665329 | | | 603232 | |
| TRU Consumption Rate (kg/cycle) | | | | | | | | | |
| Pu | 262 | 420 | 270 | 230 | 372 | 238 | 255 | 408 | 262 |
| MA | 36 | 59 | 36 | 32 | 53 | 32 | 35 | 57 | 35 |
| EOEC TRU Enrichment (w/o) | 34.4 | 36.9 | 35.4 | 30.5 | 32.5 | 31.3 | 33.6 | 35.8 | 34.4 |
| EOEC Pu Enrichment (w/o) | 29.8 | 31.7 | 30.6 | 26.6 | 28.2 | 27.3 | 29.1 | 30.9 | 29.8 |
| EOEC MA Enrichment (w/o) | 4.64 | 5.15 | 4.81 | 3.87 | 4.30 | 4.01 | 4.47 | 4.94 | 4.62 |
| EOEC TRU loading | 4949 | 5095 | 4988 | 5028 | 5185 | 5075 | 4980 | 5117 | 5015 |
| EOEC Pu Weight Fraction | | | | | | | | | |
| Pu-238 | 4.8 | 5.0 | 4.8 | 4.5 | 4.8 | 4.5 | 4.7 | 5.0 | 4.7 |
| Pu-239 | 41.4 | 39.9 | 40.9 | 43.6 | 42.1 | 43.1 | 4.21 | 40.6 | 41.6 |
| Pu-240 | 36.4 | 37.0 | 36.5 | 35.6 | 36.2 | 35.7 | 36.1 | 36.7 | 36.2 |
| Pu-241 | 6.7 | 6.8 | 6.9 | 6.3 | 6.4 | 6.5 | 6.6 | 6.7 | 6.8 |
| Pu-242 | 10.7 | 11.2 | 10.9 | 10.0 | 10.5 | 10.2 | 10.5 | 11.0 | 10.7 |

With regard to the TRU burning capability, the use of high TRU enrichment is mandatory. Since the same void reactivity is achievable with higher TRU w/o for the pan-shape core, this core has the maximum TRU burning potential, while the annular core has the minimum. The homogeneous core has a comparable performance to the pan-shape core at the expense of added complexities originating from the usage of two enrichment zones.

The effects of fuel cycle batches and fuel cycle length show up in the resulting burnup reactivity swing, discharge burnup, peak fast fluence and charge enrichment. Other performance parameters are remarkably insensitive to the fuel cycle length and batch. Extended burnup operation is strongly required for the improvement of fuel cycle economics. Annual 4-batch operations for the pan-shape and homogeneous cores are marginal, but peak fast fluence of the annular core invokes concern for the fuel clad integrity.

The neutron reaction balance shown in Table IV characterizes each design for the flooded and voided conditions. The fission neutron production rate is set to $10^5$ neutrons. The pan-shape core proves to be the highest leakage design in the flooded state. The central reflector/B4C island is insignificant in increasing the radial leakage in the flooded condition, and this leads to the usage of the lowest enrichment fuels. Due

to the low enrichment of the annular core, relatively large fraction of neutrons are captured in the fertile material to generate TRU, which in turn reduces the TRU conversion ratio and TRU burning rates.

Table IV. Neutron Reaction Balance of TRU Burner Cores at EOEC

| Core Type | Pan-Shape | | Annular | | Homogeneous | |
|---|---|---|---|---|---|---|
| State | Flood | Void, Δ | Flood | Void, Δ | Flood | Void, Δ |
| Fission | 33406 | -395 | 33507 | -389 | 33448 | -387 |
| Capture | 26464 | -3236 | 28192 | -3526 | 26706 | -3216 |
| Leakage | 40053 | 3119 | 38236 | 3413 | 39803 | 3101 |
| Radial Leakage | 14701 | 180 | 11532 | 236 | 11829 | -201 |
| Axial Leakage | 25353 | 2939 | 26704 | 3177 | 27975 | 3303 |
| SUM | | -511 | | -503 | | -502 |

Overall, the pan-shape core exhibits a slight improvement in several aspects of performance parameters such as peak neutron flux and the amount of TRU burning as well as the reduction of burden for reprocessing and manufacturing due to the fuel volume reduction. The increased number of control rods and their eventual shallow insertion at BOEC is expected to compensate for the disadvantageous high burnup swing. One attractive feature of the annular core and the pan-shape core is that they allow the use of single enrichment feed fuels, although the pan-shape core requires higher TRU enrichment feed by 4.3~4.9w/o, compared with that of the annular core. The homogeneous core has the inherent advantage of not requiring any significant core design alteration from that of the conventional breakeven core. The radial power distribution of the annular core at all rods out is peaky in the center of annular fuel ring, while those of the homogeneous core and the pan-shape core are relatively flat over the large core regions.

## 4.2 REACTIVITY COEFFICIENTS

Each core was developed to result in –0.5% at EOEC of annual 3-batch core when the flowing sodium is assumed to be voided in the driver fuel assemblies, including the lower reflector/shield and upper fission gas plenum. The change of neutron reaction balance when the flowing sodium is voided, is shown in Table IV. The predominant effect of voiding is seen in the reduced capture reaction rate and enhanced leakage. The reduction of capture reaction rate increases the fission to capture reaction rate ratio, which occurs when the spectrum is hardened. Most of MA included in the fuel tend to increase their fission to absorption cross section ratios, due to the lower threshold fission energy and large number of neutrons released (3.5~4.0) per fission than U-238. The positive reactivity introduction by 0.8 w/o higher content of MA for the pan-shape core is small compared with the reactivity added by 3.9 w/o higher content of U-238 for the annular core, and thus the annular core exhibits the greatest spectrum effect as is seen by the greatest reduction in the capture reaction rate. The reaction rate change for the pan-shape core and the homogeneous core are almost identical. This observation no longer applies when the reaction rate change is transformed into the reactivity component by the perturbation theory, due to a dissimilar adjoint spectrum.

Reactivity feedback effects caused by the flowing sodium voiding alone and Doppler broadening as well as control rod worths at BOEC and EOEC are provided in Table V. Even with the extremely flat core design, the active core voiding alone still contributes to a positive reactivity between 1030 and 1149pcm. The achievement of a zero sodium void reactivity for the active core would force a significant increase in the sodium volume fraction, combined with the introduction of spectrum softening materials. Until the void expands beyond the active core, the design provisions are not in effect. The additional fission gas plenum voiding makes the void reactivity remain slightly positive. At BOEC, the active core void reactivity of the rodded condition would be less positive than that of the unrodded condition shown in the

Table V. Reactivity Coefficients of TRU Burner Cores

| | Pan-Shape | | | Annular | | | Homogeneous | | |
|---|---|---|---|---|---|---|---|---|---|
| Number of Cycles (Batches) | 3 | 3 | 4 | 3 | 3 | 4 | 3 | 3 | 4 |
| Cycle Length (month) | 12 | 18 | 12 | 12 | 18 | 12 | 12 | 18 | 12 |
| BOEC | | | | | | | | | |
| Sodium Void Reactivity (pcm) | | | | | | | | | |
| Active Core | 918 | 918 | 925 | 949 | 959 | 964 | 967 | 968 | 980 |
| + Fission Gas Plenum | 72 | 111 | 80 | 105 | 152 | 122 | 97 | 134 | 110 |
| + Lower Reflector/Shield | -543 | -469 | -529 | -546 | -469 | -526 | -546 | -477 | -531 |
| Iso. Temp. Coeff. ($10^{-3}$ TΔρ/ΔT) | -1.72 | -1.49 | -1.65 | -1.94 | -1.72 | -1.88 | -1.76 | -1.54 | -1.70 |
| Control Rod Worth (%Δρ) | 12.9 | 12.2 | 12.7 | 9.9 | 9.4 | 9.8 | 10.0 | 9.6 | 10.0 |
| Stuck Rod Worth (%Δρ) | 0.96 | 0.92 | 0.96 | 1.02 | 0.98 | 1.03 | 0.76 | 0.73 | 0.76 |
| EOEC | | | | | | | | | |
| Sodium Void Reactivity (pcm) | | | | | | | | | |
| Active Core | 1030 | 1094 | 1042 | 1072 | 1149 | 1091 | 1102 | 1171 | 1116 |
| + Fission Gas Plenum | 129 | 205 | 142 | 180 | 279 | 201 | 176 | 254 | 190 |
| + Lower Reflector/Shield | -514 | -420 | -497 | -506 | -403 | -482 | -505 | -415 | -490 |
| Iso. Temp. Coeff. ($10^{-3}$ TΔρ/ΔT) | -1.85 | -1.69 | -1.79 | -2.07 | -1.90 | -2.01 | -1.90 | -1.74 | -1.84 |
| Control Rod Worth (%Δρ) | 13.3 | 12.9 | 13.2 | 10.3 | 10.0 | 10.2 | 10.8 | 10.6 | 10.8 |
| Stuck Rod Worth (%Δρ) | 1.05 | 1.04 | 1.05 | 1.12 | 1.13 | 1.13 | 0.82 | 0.81 | 0.82 |

table, since the increased absorption in control rods compensates for the positive reactivity effect due to the spectrum hardening. As burnup proceeds, the neutron spectrum becomes softened. However, the active core sodium void reactivity becomes more positive because the weight fraction of U-238 increases and that of Pu-239 decreases, and these two trends add positive reactivity upon the void formation. Therefore, the least negative or most positive sodium void reactivity are always found at EOEC. The fuel cycling scheme also affects the EOEC sodium void reactivity. As the batch number is increased, the EOEC MA content increases and equilibrium cycle Pu quality is degraded. These two effects result in the positive reactivity introduction. The same reasoning applies to longer cycle length operation.

The sodium void reactivity from the direct flux calculation consists of the four underlying mechanisms in the view point of perturbation theory : spectrum hardening, increased leakage, neutron capture reduction in the sodium and reduced self-shielding. Since the calculated sodium void reactivity is alike, the breakdown of reactivity from the eigenvalue difference method would be helpful to characterize each design concept. Table VI shows the breakdown of reactivity into four components and two regions when the sodium is voided at the EOEC of annual 3 batch core. The multipoint perturbation formalism developed in reference 6 is used for this purpose. Since there is no discern between the inner and outer core for the annular core, the core regions are defined to preserve the inner core (IC) to outer core (OC) volume ratio of the pan-shape core. While the sodium void reactivity is largely a net result of competition

Table VI. Sodium Void Reactivity (pcm) Component of TRU Burner Cores at EOEC

| Core Type | Pan-Shape | | | Annular | | | Homogeneous | | |
|---|---|---|---|---|---|---|---|---|---|
| Region | IC | OC | SUM | IC | OC | SUM | IC | OC | SUM |
| Spectrum | 1082 | 1006 | 2088 | 1133 | 1173 | 2305 | 1335 | 859 | 2193 |
| Leakage | -1410 | -1360 | -2770 | -1449 | -1544 | -2993 | -1688 | -1173 | -2861 |
| Radial Leakage | 74 | -345 | -271 | -195 | -221 | -416 | -138 | -33 | -171 |
| Axial Leakage | -1484 | -1015 | -2499 | -1254 | -1323 | -2577 | -1550 | -1140 | -2689 |
| Self-Shielding | 46 | 72 | 118 | 59 | 74 | 133 | 52 | 60 | 112 |
| Na Capture | 23 | 22 | 45 | 23 | 26 | 49 | 27 | 20 | 46 |
| Sodium Void Reactivity | -259 | -259 | -518 | -235 | -272 | -507 | -274 | -234 | -509 |

between spectrum hardening and increased leakage, both the spectrum and leakage components are the minimum for the pan-shape core. The smallest spectrum component of the pan-shape core is partially related with the high TRU enrichment which reduces the spectrum hardening by the increased fission in U-238. Although the EOEC TRU enrichment of the homogeneous core resembles that of the pan-shape core, the spectrum effect of the homogeneous core is midway between the pan-shape core and the annular core. The high leakage rate of the fast neutrons are also partially included in the spectrum effect through the reduced adjoint spectrum gradient versus the neutron energy. This phenomenon also works for the reduction of the spectrum effect in the pan-shape core. A relatively large self-shielding effect of the annular core may be originating from the reduction of U-238 self-shielding. The largest positive spectrum effect of the annular core is counter-balanced by the largest negative leakage effect. This asserts the effectiveness of the central reflector/$B_4C$ island that causes slight enrichment increase in normal operation and provides effective means to control the sodium void reactivity. The annular core appears to be well suited for the sodium void reactivity control of the tall breeder core where TRU is regarded as valuable resource for energy production.

Although the three core designs have the similar sodium void reactivity for the whole core void, the local sodium void effect is different among the designs. Figure 2 shows that the three designs at EOEC for annular 3-batch operation have different local void effects as the void progressively propagates from the innermost assembly ring toward the outer core. The initial large positive reactivity is merely the effect of cross section tableset change to the voided condition. Therefore, the relative increment of the reactivity and its sign are meaningful. For the whole assembly void, the local sodium voiding causes a negative reactivity insertion everywhere for any core configuration. The local void reactivity of the pan-shape core reduces at the greatest rate. For the active core plus fission gas plenum void propagation, the core reactivity increment of the pan-shape core is negative except rings 10 and 11. For the homogeneous core, the void propagation adds core reactivity up to the eighth ring, and thus the local void will propogate within this region. This local sodium void reactivity behavior can be translated into the allowance that the position of maximum corewide pin peak of the pan-shape core can be located anywhere, while the two-region homogeneous core typically requires the occurrence of maximum pin peak in the outer region of the core.

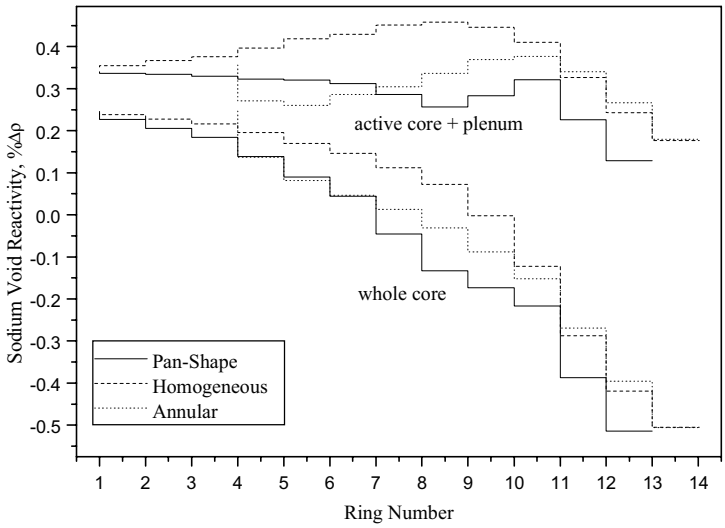


Figure 2. Local Sodium Void Reactivity Variation

The behavior of isothermal temperature coefficients (ITC) due to the dominant fuel Doppler broadening over structural material are very small, which is a typical characteristic of metal-fuelled cores and flat burners without blankets. Although each of the U-238 and Pu-240 absorption resonances remains distinctive up to about 150 and 40 keV, respectively, Doppler broadening in the resolved energy region remains only up to about 10 and 4 keV. In the current design, there is simply no appreciable neutron population whose energy is less than 9.113 keV (percents of neutron flux are 2.30 and 2.39 for BOEC and EOEC, respectively, of the annual 3-batch pan-shape core). Combined with the spectrum softening toward

EOEC, the relative absorption fraction of U-238 increases as burnup proceeds. These two aspects contribute to more negative temperature coefficients. The ITC of the pan-shape core is less negative than that of the annular core and this originates from the fact that the U-238 weight fraction is small in the pan-shape core. The examination of Table V suggests that the U-238 weight fraction is critical in determining the ITC of any specific design and cycle scheme.

The Doppler defect of each design for annual 3-batch operation is broken down into the reactivity component by the perturbation theory as is shown in Table VII. The Doppler defect cited is the reactivity change when the fuel region temperature is raised from 850K to 1150K. The increased absorption of neutrons is the main reason for negative fuel temperature coefficients. However, it is partially compensated for by the reduced leakage. The pan-shape core that is the most leaky design in the flooded condition, has the most positive leakage effect. In cores with a high neutron leakage in the reference state, the leakage is reduced significantly as the fuel temperature rises. This fact means that a pancake core with a high neutron leakage rate will inevitably confront the added difficulty in increasing negative reactivity feedback by Doppler broadening.

Table VII. Doppler Defect Component of TRU Burner Cores

| | Pan. | Annular | Homo. |
|---|---|---|---|
| Spectrum | -1 | -1 | -1 |
| Radial Leakage | -50 | -77 | -84 |
| Axial Leakage | 59 | 84 | 91 |
| Production | 4 | 3 | 4 |
| Absorption | -65 | -72 | -65 |
| Total, pcm | -53 | -63 | -55 |

The spectrum softening toward EOEC and the competing absorption material reduction (especially fissile material burnup) against the control rods make the total control rod worth higher toward EOEC. The most reactive stuck rod worths at BOEC are around 0.73~1.03 $\%\Delta\rho$ for any configuration and cycle scheme. Therefore, the N-1 rod worths remain large enough to control the BOEC excess reactivities and power defect. The largest margin to the reactivity control requirement is identified for the pan-shape core.

## 5. CONCLUSIONS

Three different TRU burner cores with the same low sodium void reactivity were compared in their design features, neutronic performance parameters and reactivity coefficients. Depending on the core concepts, the enrichment requirement, TRU burning capability and sodium void reduction mechanism are different. When the three designs are subjected to the different batch and long cycle length operation, the performance parameters show no significant degradation except the burnup reactivity swing and peak fast fluence.

It is shown that the usage of the variable fuel length in the pan-shape core allows the core compaction, compared with the annular core (13.6%) and homogeneous core (3.0%). In addition, the pan-shape core saves 36 driver fuel assemblies over the homogeneous core. This will lead to the savings in the fuel reprocessing burden and fabrication cost, and allow a compact reactor vessel design.

The pan-shape core accepts the single enrichment feed and shows a relatively flat power distribution. A sufficient negative sodium void reactivity is achieved though the extreme pancaking of the inner core and this core is capable of further reducing the sodium void reactivity once the benefit of the core compactness is sacrificed. The TRU burning characteristics are the highest among the three designs. In addition to these attractive design features, this design appears to open up the potential of eliminating the barrier by the nuclear proliferation concerns, once the reprocessing technology that blends only the TRU and fertile materials becomes available.

## ACKNOWLEDGMENTS

The authors are grateful to Robert N. Hill (ANL) for his kind release of information on the fueled assembly specifications of the '96 OECD/NEA burner benchmark core. This work was supported by Nuclear R&D Long-Term Development Program of the Ministry of Science and Technology of Korea.

## REFERENCES

1. H. S. Khalil, R. N. Hill, "An Evaluation of Liquid Metal Reactor Design Options for Reduction of Sodium Void Worth," Nuclear Science and Engineering, Vol. 109, pp. 221-266, 1991.

2. R. N. Hill, "LMR Design Concepts for Transuranic Management in Low Sodium Void Worth Cores," Proceedings, International Conference on Fast Reactor and Its Fuel Cycle," Kyoto, Japan, Vol. II, pp. 19.1-1-11, 1991.

3. W. Maschek, D. Thiem, G. Heusener, "Safety Features of a Reactor Core with Minor Actinide Transmutation and Burning Capabilities," GLOBAL '99, Jacksonhole, U.S.A., 1999.

4. H. B. Choi, T. J. Downar, "The Neutronics Analysis of a Liquid Metal Reactor for Burning Minor Actinides," Proceedings, International Conference on Design and Safety of Advanced Nuclear Power Plants, Tokyo, Japan, Vol.1, pp. 5.5-1-6, 1992.

5. OECD Documents, "Physics of Plutonium Recycling. Volume V – Plutonium Recycling in Fast Reactors", OECD, 1996.

6. S. J. Kim, N. Z. Cho, Y. J. Kim, "A Pan-Shape Transuranic Burner Core with a Low Sodium Void Worth," Annals of Nuclear Energy, (in press).

7. J. D. Kim, C. S. Gil, "KAFAX-F22: Development and Benchmark of Multi-group Library for Fast Reactor Using JEF-2.2," KAERI/TR-842/97, KAERI, 1997.

8. R. E. MacFarlane, "TRANSX 2: A Code for Interfacing MATXS Cross-Section Libraries to Nuclear Transport Codes," LA-12312-MS, LANL, 1993.

9. R. E. Alcouffe, et al., "User's Guide for TWODANT," LA-10049-M, LANL, 1990.

10. B. J. Toppel, "The Fuel Cycle Analysis Capability REBUS-3," ANL-83-2, ANL, 1983.

11. K. L. Derstine, "DIF3D," ANL-82-64, ANL, 1984.